Paper No. 91-025

AAS Guidance and Control Conference
Keystone, Colorado, February 2–6, 1991

AUTONOMOUS, ALL-STELLAR ATTITUDE DETERMINATION EXPERIMENT: GROUND TEST RESULTS

H. L. Fisher, T. E. Strikwerda, C. C. Kilgus
L. J. Frank, and M. D. Shuster*

An all-stellar instrument has been designed to demonstrate five-arc-second autonomous attitude determination on a NASA Spartan spacecraft. The instrument includes a Charge-Coupled Device (CCD) star camera that provides centroid measurements of up to five simultaneous star images with an update rate of 10 per second. At slue rates less than 0.1 degrees per second the camera accuracy varies from 5 to 15 arc seconds per image, depending on star magnitude. The instrument processor matches measured stars with a 9000 entry catalog and then computes a single-frame and Kalman-filter estimate of Spartan attitude and attitude rate each second. By using multiple star images for attitude determination, an accuracy of a few arc seconds can be obtained. The performance of the camera and processing techniques have been studied in an extensive modeling and test program including star measurements taken under realistic conditions at the Jet Propulsion Laboratory Table Mountain Observatory. Detailed results of these tests are presented.

INTRODUCTION

The star-tracker instrument (START) described in this paper was developed to test a new CCD-based star camera and a real-time technique for star identification and attitude determination. Both the instrument and star identification methods have been described in previous papers;[1,2] these will be reviewed briefly here. In this paper we concentrate on several methods which have been developed for evaluating the accuracy of the camera's star measurements and the performance of the attitude determination techniques when observing real stars. Algorithms for evaluating the data and results from several test cases are presented and discussed.

Tests under realistic conditions are useful, because camera performance tests in the laboratory are limited typically to one test source or a grid of sources and precise motion of the test sources or camera is difficult. Test sources may not accurately simulate the true image profile, size or spectral characteristics. In addition, the software for attitude determination cannot be adequately tested with these sources; simulated data or actual star observations are required.

The flight test of the instrument is expected in 1993. The Spartan spacecraft, built by NASA Goddard Space Flight Center and funded by the U. S. Air Force, will be deployed from the shuttle for a 40-hour preprogrammed mission that will include sluing and staring observations.[1] The instrument will then be retrieved for possible upgrades leading to sub-arc-second performance.

*The Johns Hopkins University Applied Physics Laboratory, Johns Hopkins Road, Laurel, MD 20723-6099

STAR CAMERA INSTRUMENT

The START instrument consists of a CCD star camera and its electronics and processor package, the instrument flight processor for data collection, attitude determination and instrument control, the power distribution system, and support structure.

CCD Star Camera

The CCD camera, built by Hughes Danbury Optical Systems, has a 7.2 deg × 9 deg field of view (FOV) and a 256 pixel × 403 pixel CCD array. Ten frames per second of digitized CCD data are sent to the camera processor, which computes image plane coordinates for up to five stars in each frame, corrects for various effects such as radial distortion, and sends the data to the flight processor. In the event there are more than five stars in one frame, an algorithm attempts to select five stars that are somewhat distributed throughout the FOV.

Instrument Flight Processor

The instrument processor has three main functions. Its highest priority is to collect all camera data, format it, and send it to the Spartan. The second function is to receive and act on preprogrammed commands from Spartan for instrument control. When there is time remaining after these tasks finish, the processor is used by attitude-determination software to process as many camera frames as possible. This task determines attitude by identifying stars in the FOV and then computing the optimal attitude estimate from the inertial frame to camera frame. The attitude results are stored on the tape recorder along with the camera data for later ground analysis; they are not used in the Spartan control system.

Star Identification

The technique for star identification follows closely that of Junkins and Strikwerda.[3] First, the angle between a pair of measured stars is compared with the angle between candidate pairs of catalog stars. This comparison is repeated using different pairs of measured stars until a possible match is found. The rotation matrix from the catalog frame to the camera frame is then computed (see below) and image-plane coordinates of other catalog stars are computed and checked to determine if they match other measured stars. Matches of at least three stars are required to confirm the identification. The attitude estimate can then be refined using all the identified stars.

The on-board catalog for this mission contains about 9000 stars. In sparse regions of the sky it is complete to approximately 6.0 visual magnitude. In dense regions some faint stars in this range have been eliminated. Although 9000 stars appear to be more than enough, it must be kept in mind that in dense regions the camera's star selection algorithm may not always select the brightest stars, but rather those with a good spatial distribution. Thus, to better "guarantee" a match for most camera orientations, we need a large catalog. In addition, we plan to test the camera and software performance when the CCD upper threshold is set to a lower value (fainter magnitude). This will require fainter stars in the catalog.

Our attitude determination software requires an *a priori* attitude estimate to avoid having to search the entire catalog. This estimate is provided by preprogrammed commands from Spartan's maneuver timeline.

Attitude Determination

If measured stars are matched with catalog stars, several methods exist to calculate the transformation, or camera attitude, between the catalog frame and the camera frame. The most intuitive is the Triad method,[4,5] a simple algorithm which estimates attitude from only two stars. A more general algorithm is QUEST,[5] which determines the attitude using any quantity of star-direction data.

Successive attitude estimates can be used to estimate the camera angular rate. Again, two methods exist for this calculation. The straightforward technique is to compute finite differences of the attitude and divide by the time. However, this method can be very inaccurate if the time interval is short. A Kalman filter was developed to produce a more accurate estimate of attitude and attitude rate.[6]

GROUND TEST METHODS

Two methods were developed for evaluating the camera and attitude determination performance with real star data: Earth-fixed tests and sluing tests. Our first Earth-fixed tests were conducted at the Applied Physics Laboratory (APL) and were valuable for end-to-end functional testing of the overall instrument and for performance testing of the camera and attitude software. We later tested the camera at Jet Propulsion Laboratory's Table Mountain Observatory (TMO) using both Earth-fixed and sluing tests.

Earth-Fixed Tests

Earth-fixed tests consist of holding the camera in a fixed, vertical orientation and letting the stars drift through the FOV. The constant rotation of the Earth causes the stars to pass through the FOV slowly and smoothly. Using the analysis discussed in a later section, it is possible to examine errors on both a pixel and FOV scale as well as frame-to-frame accuracy of the camera and attitude determination. Earth-fixed tests are relatively easy to conduct and quite useful for detecting high-spatial-frequency errors.

Our original test configuration used for testing the entire instrument consisted of the camera in a special enclosure with an optical window and a nitrogen purge port, instrument flight processor, and the instrument ground support equipment (GSE). The GSE serves primarily to emulate the Spartan for both instrument commanding and data logging. The camera, in its enclosure, was placed outside and pointed vertically to minimize errors due to atmospheric refraction. Meanwhile, the instrument processor and GSE collected and processed data. This test verified overall function, control, and measured throughput of camera, flight processor, and GSE. With this arrangement we were able to operate the instrument in a realistic way and verify that the attitude determination software was properly identifying stars and computing attitude.

Our camera performance evaluation was hampered, however, by poor atmospheric transparency and by being limited to only one slue rate (Earth rate). The rate of star motions is far too slow to be representative of most space applications of this technology. These limitations led us to develop more comprehensive tests and analysis techniques for the second method of testing at TMO.

Sluing Tests

The second phase of testing was carried out at TMO. The camera and enclosure were mounted to the side of a 24-inch telescope which provided a stable mounting, when the drive was off, for the Earth-fixed observations, and, with its sidereal and sluing capability, provided various slue rates about one or both axes to simulate motion of a spacecraft. Data were collected with a portable computer (eliminating the need to transport the entire instrument and GSE) and all data processing and analysis were performed off-line.

The TMO tests were conducted primarily for camera performance evaluation but also provided additional data for analyzing the attitude determination methods. Attitude performance will change as camera performance degrades with faster slue rate. However, testing the camera on a moving platform presents special problems not encountered with Earth-fixed tests. One of the primary concerns was how steady the telescope would be as a platform. Although direct measurements were not made, visual checks through the telescope indicated that the telescope drive motion was quite smooth. Also, from the data that has been processed, position errors between stars do not appear to be correlated.

Another problem is atmospheric refraction, both total and differential. While most of our data segments were short and taken with the telescope nearly vertical to minimize refraction effects, the higher rate slues subtended a sufficiently large arc that refraction could be a problem. No corrections were made for refraction although it could be handled without too much additional processing.

The Table Mountain experiments also presented the opportunity to test the camera sensitivity at a site with very good atmospheric transparency, or low extinction. Collecting data at a low extinction site gives a better indication of how the camera will perform in space. The extinction at TMO is typically 0.1 magnitude, which is very good. We believe extinction was at least that low during our tests, based on our extinction data. To further characterize the camera sensitivity several minutes of data were collected with and without the protective glass window on the enclosure. Without the window the signal increased by approximately 0.20–0.25 magnitude.

TEST-DATA PROCESSING

Data processing for these ground tests requires several steps: 1) identification of the measured stars, 2) computation of the single-frame and Kalman-filter estimates of attitude, 3) estimation of the camera slue axes and rates to obtain a reference attitude history, 4) computation of ideal star positions or paths on the CCD based on the calculated reference attitude, and 5) computation of residuals between measured and computed positions. The star position residuals can reveal interpolation errors, quantization errors and large scale image plane errors. Comparisons between the reference attitude and single-frame or Kalman-filter attitude estimates shows attitude determination performance.

Star Identification

Except for the end-to-end functional tests of the entire instrument, data processing is performed off-line. The first step is to identify stars as mentioned above.[3] The output of this process is a table consisting of six columns and n rows, one for each frame. Each row of the table consists of the frame time reported by the camera, followed by as many as five catalog star identification numbers, one for each measured star, if it was identified in that frame. This table was the point of reference for the following processing steps and avoided the problem of having to reexecute the star-identification program when different reduction techniques or parameters are tested.

Data-Processing Method

A method to estimate the errors in the star measurements and in the attitude estimates from the on-board software is highly desired. Ideally, this method would be able to independently measure the attitude of the camera in order to obtain a true reference from which to measure the errors. Unfortunately, there was no method available to measure the attitude of the camera to an accuracy greater than that provided by the measurements themselves. Therefore, the data itself must be used somehow to estimate a reference attitude that is, hopefully, more accurate than the estimate from the on-board attitude-determination software. To do this, models of the camera motion were constructed that exploit the characteristics of the tests. For the Earth-fixed case, it was assumed that the camera is rigidly attached to the Earth, and therefore the motion of the camera is due solely to the rotation of the Earth, which is well known. For the telescope slue case, it was assumed that the telescope drive rate is constant,

and that the motion of the camera is due to the combined rotation of the Earth and of the telescope drive. The tests were carefully set up and performed to eliminate as much as possible any vibrations or other disturbances that would violate these assumptions.

A maximum-likelihood estimator has been developed for the camera motion. Given a set of n star measurements, the kth star measurement obeys the following relation

$$\hat{\mathbf{W}}_k = R_{\text{Cam}\leftarrow I}(t_k)\,\hat{\mathbf{V}}_k + \Delta\hat{\mathbf{W}}_k \quad , \tag{1}$$

where $\hat{\mathbf{V}}_k$ is a unit vector representing the star direction in the inertial coordinate system (obtained from the star catalog), $\hat{\mathbf{W}}_k$ is the corresponding unit vector representing the measured direction of the star in the camera coordinate system, t_k is the time of the measurement, $R_{\text{Cam}\leftarrow I}(t_k)$ is the attitude matrix at that time, and $\Delta\hat{\mathbf{W}}_k$ is the measurement error, which is assumed to be Gaussian with

$$E\{\Delta\hat{\mathbf{W}}_k\} = 0 \quad , \quad E\{\Delta\hat{\mathbf{W}}_k\Delta\hat{\mathbf{W}}_k^T\} = \sigma_k^2\left(I - \hat{\mathbf{W}}_k\hat{\mathbf{W}}_k^T\right) \equiv R_k \quad . \tag{2}$$

Although some of the error components, such as quantization error, are not Gaussian, the total error is reasonably close to Gaussian.

For the Earth-fixed case, the attitude can be written as a sequence of two rotations: a rotation from the inertial system to an Earth-fixed system, and a rotation from the Earth-fixed system to the camera coordinate system, as follows:

$$R_{\text{Cam}\leftarrow I}(t) = R_{\text{Cam}\leftarrow E}\,R_{E\leftarrow I}(t) \quad . \tag{3}$$

The first rotation is time-varying due to the Earth's rotation. The second is assumed to be constant, i.e., the camera is assumed to be rigidly fixed to the Earth. Any Earth-fixed coordinate system may be chosen, which need not be aligned with any "natural" axes of the Earth. In fact, a somewhat unnatural choice will be made in order to simplify the equation. With this in mind, Eq. (3) is rewritten with the rotation matrices expressed as functions of rotation vectors, as follows:

$$R_{\text{Cam}\leftarrow I}(t) = R^T(\boldsymbol{\theta})\,R(\boldsymbol{\omega}_E(t - t_o)) \quad , \tag{4}$$

where $\boldsymbol{\omega}_E$ is the angular velocity vector of the Earth's rotation, t_o is the time of the first measurement, and $\boldsymbol{\theta}$ is a constant rotation vector representing the rotation from the camera coordinate system to the Earth-fixed system. In writing this equation the Earth-fixed coordinate system has been implicitly chosen to be the one which is aligned with the inertial coordinate system at time t_o. Thus, the z-axis of our Earth-fixed system is aligned with the polar axis, as usual, but the x-axis is not necessarily aligned with Greenwich. Also, $R^T(\boldsymbol{\theta})$ is necessarily the star camera attitude at time t_o.

Substituting the kinematic model of Eq. (4) into the measurement model of Eq. (1) results in

$$\hat{\mathbf{W}}_k = R^T(\boldsymbol{\theta})\,R(\boldsymbol{\omega}_E(t_k - t_o))\,\hat{\mathbf{V}}_k + \Delta\hat{\mathbf{W}}_k \quad , \tag{5}$$

which can be written as

$$\hat{\mathbf{W}}_k = R^T(\boldsymbol{\theta})\,\hat{\mathbf{V}}_k^E + \Delta\hat{\mathbf{W}}_k \quad , \tag{6}$$

where

$$\hat{\mathbf{V}}_k^E = R(\boldsymbol{\omega}_E(t_k - t_o))\,\hat{\mathbf{V}}_k \tag{7}$$

is the direction of the star in the Earth-fixed coordinate system. From Eq. (6) then, we see that the attitude estimation problem consists of finding the rotation matrix $R^T(\boldsymbol{\theta})$ which best transforms the set of vectors $\hat{\mathbf{V}}_k^E$ into the set $\hat{\mathbf{W}}_k$. This can be accomplished with the QUEST algorithm.[5]

Once $R(\boldsymbol{\theta})$ has been estimated, the attitude at any time can be computed using Eq. (4). This attitude can be used as a reference for computing errors in the attitude estimates provided by the on-board software.

The reference attitude can be used also to obtain estimates of individual star measurement errors. Note that $R^T(\theta)\hat{\mathbf{V}}_k^E$ would be the position in the camera system of the kth star, if our attitude estimate was error free. Thus $\hat{\mathbf{W}}_k - R^T(\theta)\hat{\mathbf{V}}_k^E$ is an estimate of $\Delta\hat{\mathbf{W}}_k$, the error in the kth measurement. Because the camera is likely to measure a given star multiple times as it moves across the field of view, a time history of the measurement errors for that star can be constructed.

Camera Slue Analysis

The Earth-fixed case is extended to the single-axis-telescope-slue case by adding another intermediate reference frame, one that is fixed in the telescope. The telescope is assumed to cause the telescope to rotate with a constant angular velocity with respect to the Earth. Thus, another time-varying rotation is added to the sequence of rotations as follows,

$$R_{\text{Cam}\leftarrow I}(t) = R_{\text{Cam}\leftarrow\text{Tel}}\, R_{\text{Tel}\leftarrow E}(t)\, R_{E\leftarrow I}(t) \tag{8}$$

$$= R^T(\theta)\, R(\omega_{\text{Tel}}(t-t_o))\, R(\omega_E(t-t_o)) \quad , \tag{9}$$

where ω_{Tel} is the angular velocity of the telescope drive with respect to the Earth. Again, this equation is substituted into Eq. (1) and the catalog star positions transformed from the inertial frame to the Earth-fixed frame, resulting in

$$\hat{\mathbf{W}}_k = R^T(\theta)\, R(\omega_{\text{Tel}}(t_k - t_o))\, \hat{\mathbf{V}}_k^E + \Delta\hat{\mathbf{W}}_k \quad . \tag{10}$$

We now have a set of nonlinear equations in both θ and ω_{Tel}, and we cannot use the QUEST algorithm as in the Earth-fixed case. Instead, we will use a perturbation method to arrive at a solution. First, let us rewrite the remaining rotation matrices as matrix exponentials,

$$\hat{\mathbf{W}}_k = e^{-[[\theta]]}\, e^{[[\omega_{\text{Tel}}]](t_k - t_o)}\, \hat{\mathbf{V}}_k^E + \Delta\hat{\mathbf{W}}_k \quad , \tag{11}$$

where matrices of the form $[[\,\mathbf{U}\,]]$ are anti-symmetric matrices such that $[[\,\mathbf{U}\,]]\,\mathbf{V}$ is equal to the vector cross product $\mathbf{V} \times \mathbf{U}$ (or $-\mathbf{U} \times \mathbf{V}$). Given initial estimates of θ and ω_{Tel}, denoted by θ^* and ω_{Tel}^*, we can define perturbations $\delta\theta$ and $\Delta\omega_{\text{Tel}}$ such that

$$\theta = \delta\theta \otimes \theta^* \tag{12}$$

$$\omega_{\text{Tel}} = \omega_{\text{Tel}}^* + \Delta\omega_{\text{Tel}} \quad , \tag{13}$$

where $\otimes$ denotes rotation-vector composition, so that rotation θ corresponds to the rotation represented by θ^* followed by the rotation represented by $\delta\theta$. Equivalently, in terms of rotation matrices,

$$e^{[[\theta]]} = e^{[[\delta\theta]]}\, e^{[[\theta^*]]} \quad . \tag{14}$$

Equation (11) can now be expanded in a first-order Taylor series

$$\hat{\mathbf{W}}_k = e^{-[[\theta^*]]}\,(I - [[\delta\theta]])\left(e^{[[\omega_{\text{Tel}}^*]](t_k - t_o)} + \sum_{i=1}^{3} \left.\frac{\partial e^{[[\omega]](t_k - t_o)}}{\partial \omega_i}\right|_{\omega_{\text{Tel}}^*} \Delta\omega_{\text{Tel}\,i}\right) \hat{\mathbf{V}}_k^E + \Delta\hat{\mathbf{W}}_k \quad . \tag{15}$$

Expanding, and keeping only first-order terms,

$$\hat{\mathbf{W}}_k = \hat{\mathbf{W}}_k^* + e^{-[[\theta^*]]}\left[\left[\, e^{[[\omega_{\text{Tel}}^*]](t_k - t_o)}\hat{\mathbf{V}}_k^E \,\right]\right]\delta\theta + \sum_{i=1}^{3}\left(e^{-[[\theta^*]]}\left.\frac{\partial e^{[[\omega]](t_k - t_o)}}{\partial \omega_i}\right|_{\omega_{\text{Tel}}^*} \hat{\mathbf{V}}_k^E\right)\Delta\omega_{\text{Tel}\,i} + \Delta\hat{\mathbf{W}}_k \quad , \tag{16}$$

where

$$\hat{\mathbf{W}}_k^* \equiv e^{-[[\theta^*]]} e^{[[\omega_{\text{Tel}}^*]](t_k - t_o)} \hat{\mathbf{V}}_k^E \quad , \tag{17}$$

and we have used the fact that $[[\mathbf{U}]]\mathbf{V} = -[[\mathbf{V}]]\mathbf{U}$. Thus, an effective measurement can be defined as

$$\mathbf{Z}_k = H_k \, \delta\mathbf{X} + \Delta\hat{\mathbf{W}}_k \quad , \tag{18}$$

where

$$\mathbf{Z} = \hat{\mathbf{W}}_k - \hat{\mathbf{W}}_k^* \quad , \tag{19}$$

$$\delta\mathbf{X} = \begin{bmatrix} \delta\theta \\ \Delta\omega_{\text{Tel}} \end{bmatrix}_{6\times 1} \quad , \tag{20}$$

$$H_k = [\, H_{\theta,k} \;\; | \; H_{\omega_{\text{Tel}},k} \,]_{3\times 6} \quad , \tag{21}$$

$$H_{\theta,k} = [[\hat{\mathbf{W}}_k^*]] \, e^{-[[\theta^*]]} \quad , \tag{22}$$

$$H_{\omega_{\text{Tel}},k} = e^{-[[\theta^*]]} [\, \mathbf{U}_{1,k}, \, \mathbf{U}_{2,k}, \, \mathbf{U}_{3,k} \,] \quad , \tag{23}$$

and

$$\mathbf{U}_{i,k} \equiv \left. \frac{\partial e^{[[\omega]](t_k - t_o)}}{\partial \omega_i} \right|_{\omega_{\text{Tel}}^*} \hat{\mathbf{V}}_k^E \quad . \tag{24}$$

Since the unit vector measurements have only two degrees of freedom, the measurements must be reduced to minimum dimension by using only the x and y components. The reduced measurement is given by

$$\mathbf{Z}_k' = H_k' \, \delta\mathbf{X} + \Delta\hat{\mathbf{W}}_k' \quad , \tag{25}$$

where

$$\mathbf{Z}_k' = M \, \mathbf{Z}_k \quad , \quad H_k' = M \, H_k \quad , \quad \Delta\hat{\mathbf{W}}_k' = M \, \Delta\hat{\mathbf{W}}_k \quad . \tag{26}$$

and

$$M \equiv \begin{bmatrix} 1 & 0 & 0 \\ 0 & 1 & 0 \end{bmatrix} \quad . \tag{27}$$

All of the measurements, $\mathbf{Z}_k$, $k = 1, \ldots, n$, can be stacked to form a single measurement

$$\mathbf{Z} = H \, \delta\mathbf{X} + \boldsymbol{\epsilon} \quad , \tag{28}$$

where

$$\mathbf{Z} = [\, \mathbf{Z}_1'^T, \ldots, \mathbf{Z}_n'^T \,]^T \quad , \tag{29}$$

$$H = [\, H_1'^T, \ldots, H_n'^T \,]^T \quad , \tag{30}$$

$$\boldsymbol{\epsilon} = [\, \Delta\hat{\mathbf{W}}_1', \ldots, \Delta\hat{\mathbf{W}}_n' \,]^T \quad . \tag{31}$$

The minimum variance estimate of $\delta\mathbf{X}$ is then

$$\delta\mathbf{X} = (H^T R^{-1} H)^{-1} H^T R^{-1} \mathbf{Z} \quad , \tag{32}$$

where

$$R = \begin{bmatrix} R'_1 & 0 & \dots & 0 \\ 0 & R'_2 & \dots & 0 \\ \vdots & \vdots & \ddots & \vdots \\ 0 & 0 & \dots & R'_n \end{bmatrix}_{2n \times 2n} , \tag{33}$$

$$R'_k = M\, R_k\, M^T \quad . \tag{34}$$

This perturbation can be applied to the prior estimate to obtain a new estimate of θ and ω_{Tel}. The entire process can be iterated until $\delta \mathbf{X}$ becomes sufficiently small. Usually only two or three iterations were required for the cases that we have examined. Once the final state estimate is computed, the attitude at any time is obtained from Eq. (9). An estimate of the error in the kth measurement is obtained by using the final state estimate to compute $\mathbf{Z}_k$.

RESULTS

We discuss results of three types of observations: a slue slightly faster than sidereal rate, an Earth-fixed case, and a 0.1 deg/second slue.

Delta Sidereal Slue Results

The first results that we will examine are for the star camera mounted on the telescope and slued in right ascension at a rate slightly different than sidereal rate. The rate was such that the stars moved the distance of two pixels in the x-direction during the data segment. Every sixth data frame (i.e., one frame every 0.6 sec.) was processed by the (ground-based) on-board attitude determination software to identify the stars and estimate attitude. A reference attitude history was computed and individual star residuals determined using the technique presented earlier. Figure 1 shows the residuals for star 5303 (5303 is the catalog identification number for the star). There are clearly two cycles of a sinusoidal trend in the x-residuals, with an amplitude of 5 arc seconds. This is almost certainly due to centroid interpolation error. Telescope drive errors have been ruled out as a possible cause, because residuals for another star in the same experiment have similar sinusoidal behavior but different phase. Also, residuals for a dimmer star have non-sinusoidal behavior.

Earth-Fixed Case

The next results are for an Earth-fixed case in which the camera was oriented to point toward the zenith. Data were collected for approximately 18 minutes. Every tenth data frame (i.e., one frame per second) was processed by the on-board attitude determination software to identify the stars and estimate attitude.

Figure 2 shows the tracks of the stars that were identified. A reference attitude history was computed and individual star residuals and attitude errors determined using the technique presented earlier. Figure 3 shows the residuals for star 3462. This star left the FOV at about $t = 10000$ sec, which is why there is no data after that time. The last several samples have a large x-error, probably because a portion of the star image was lying off of the usable area of the CCD. This "edge effect" is apparent in most of the cases in which a star leaves or enters the FOV. In addition to the edge effect, there may be a bias in both the x and y residuals that could be due to catalog error. Residuals for another star (5170) for this case are shown in Fig. 4. This star entered the FOV at about $t = 9650$ sec, at which point there appeared an edge effect error in x. There is also a slight downward trend in the x-residuals which may be the result of uncompensated radial distortion due to star color. The y- residuals have a somewhat sinusoidal behavior which is probably due to centroid interpolation error, since the star motion had a slight component in the y-direction which caused the star to move about 1 pixel along the y-axis.

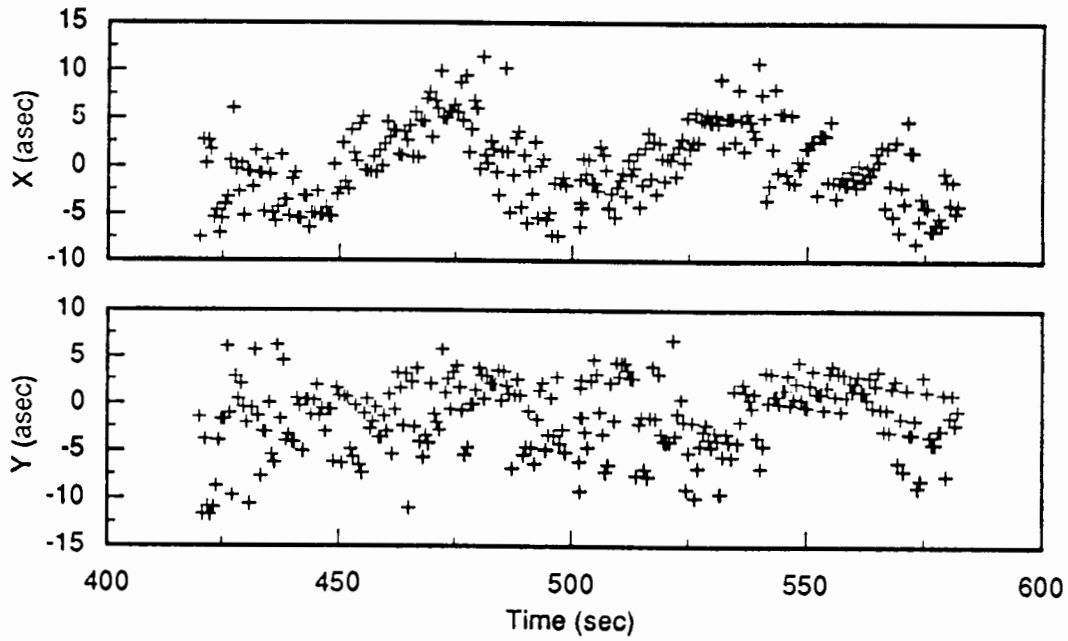

Fig. 1 Residuals for star number 5303 which moved the distance of two pixels in the x-direction. The cyclic variation in the x-residuals is probably due to interpolation error.

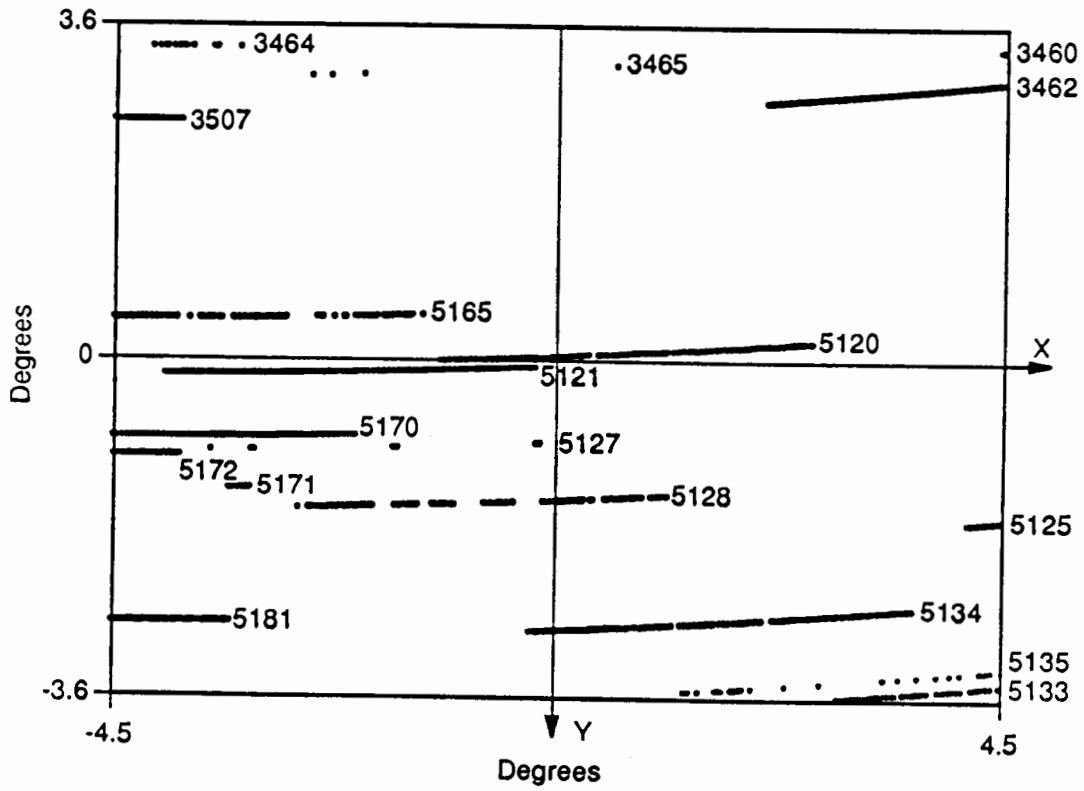

Fig. 2 Paths of stars through the FOV for an Earth-fixed case.

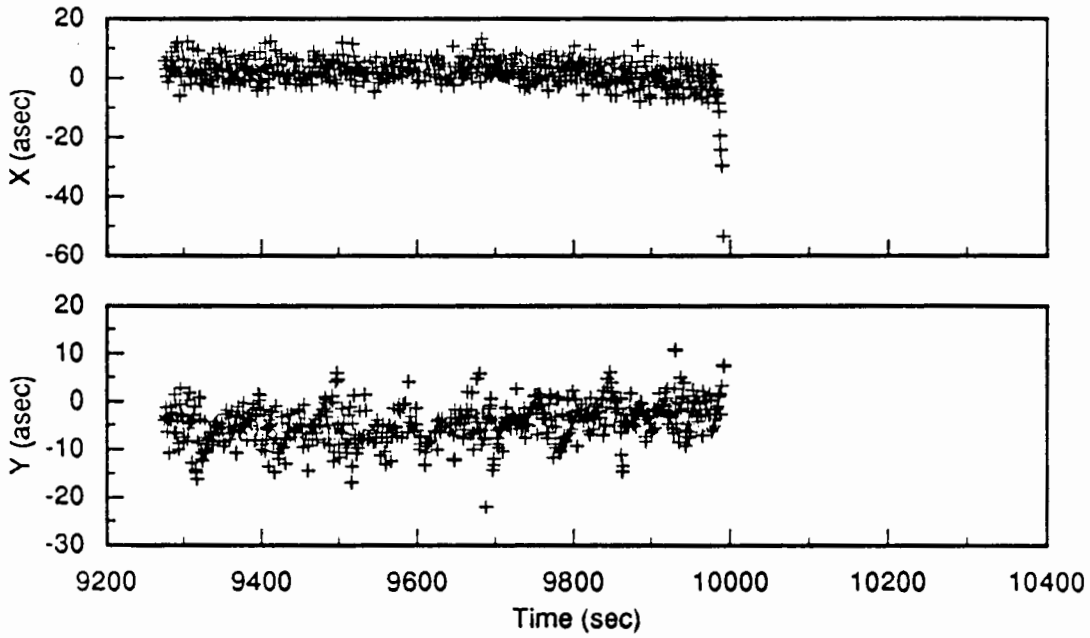

Fig. 3 Residuals for star number 3462. Note the large x-error when the star left the FOV.

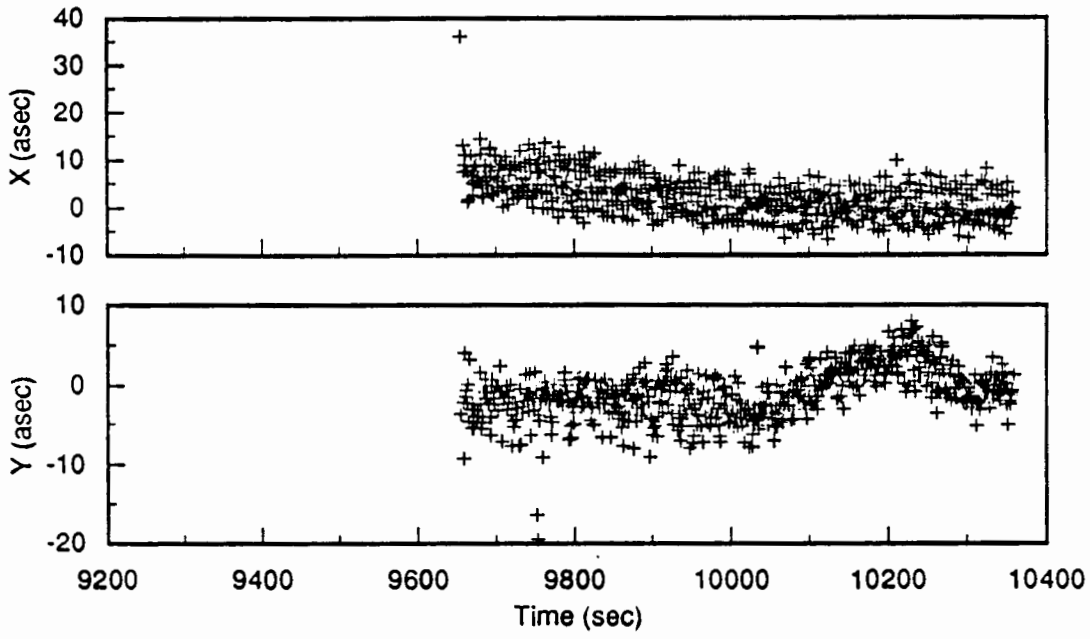

Fig. 4 Residuals for star number 5170. The slow variation in the y-residuals occurs as the star transits one row of the CCD.

In addition to the individual star residuals, we have also examined the attitude estimates from the on-board software for the Earth-fixed case. Both the single-frame attitude and the Kalman-filter attitude were analyzed by computing the small angles characterizing those attitudes as measured from the reference attitude. Results for the single-frame attitude are shown in Fig. 5. The middle portion of the data segment appears to be quieter than the beginning and end. During the middle portion there were three stars (5170, 3462, 5121) in the third to fourth magnitude range that were measured consistently. There were fewer good stars being measured at the beginning (before 5170 entered the FOV) and at the end (after 3462 left the FOV). Also, there is a noticeable spike in the attitude error at about $t = 10000$ sec, which is probably due to the edge effect error of star 3462 as it left the FOV. Not visible from this figure is the fact that between $t = 9500$ sec and $t = 9650$ sec there were many frames for which there were not enough stars identified for a confirmed match (i.e., less than three were identified). This may be because one of the stars being measured during that time may have been absent from the catalog, and the errors for others may have been too large. Except for this problem, though, the single-frame attitude estimates seem to be fairly good. Sample standard deviations of the errors were computed to be 4.5, 3.7, and 83. arc seconds, for the x, y, and z axes of the camera, respectively. These numbers are about what was expected given the errors in the individual star measurements. The z-axis (roll) is along the camera boresight. The large value for the z-axis attitude error is consistent with position errors of 5–10 arc seconds for stars several degrees from the camera boresight. Figure 6 shows the errors in the Kalman-filter attitude estimate for the same case. There is some improvement over the single-frame errors in all three axes, but the greatest improvement is in roll (z-axis). The standard deviations for the filter errors were 3.9, 3.3, and 49. arc seconds. There is some structure visible in the filter results, and to a lesser extent in the single-frame results. Although this could be due to uncompensated motion of the camera, it is more likely the result of the systematic errors in the star measurements, such as interpolation error, which change as the stars move across the FOV and also as different stars are selected.

Slue (0.1 deg/sec) *Case*

Figure 7 shows the single-frame attitude errors for a slue case. The slue was at 0.1 deg/sec in right ascension and was about three minutes long. One frame of data per second was processed. Three periods are labeled along the time axes of the plots. During the first period there were always three or four bright stars (magnitude range 3.0–4.0) in each frame. The attitude results during this period were, accordingly, very good. Then, during the second period, the brighter stars began to drop out and were replaced by dimmer stars, with more toggling (the camera selected different stars in each frame). This caused a noticeable degradation in the attitude accuracy. At the transition from the second to the third period, the number of bright stars was reduced from two to one. The single remaining bright star was measured for the remainder of the third period. However, it was moving parallel to and slowly closer to the edge of the FOV, so that it had a large edge effect error during the last several seconds of the data segment. The other stars measured during the third period were fainter. In addition, all of the stars (including the bright one) measured during that period were close together, with the largest separation of any two being about 3 degrees. All of these problems caused the attitude errors to grow even worse during the third period, especially the roll errors. Averaged over the entire data segment, however, the attitude performance was quite good. The single-frame sample standard deviations were 4.0, 4.8, and 79. arc seconds for the x, y, and z errors, respectively. Standard deviations for the Kalman-filter errors were 3.5, 3.5, and 52. arc seconds. As in the Earth-fixed case, the filter roll error shows the most improvement over the single-frame results.

The attitude errors for the 0.1 deg/sec slue case did not seem to be any larger than the Earth-fixed case. However, for a 1.0 deg/sec slue case that we processed, the errors were about twice as large.

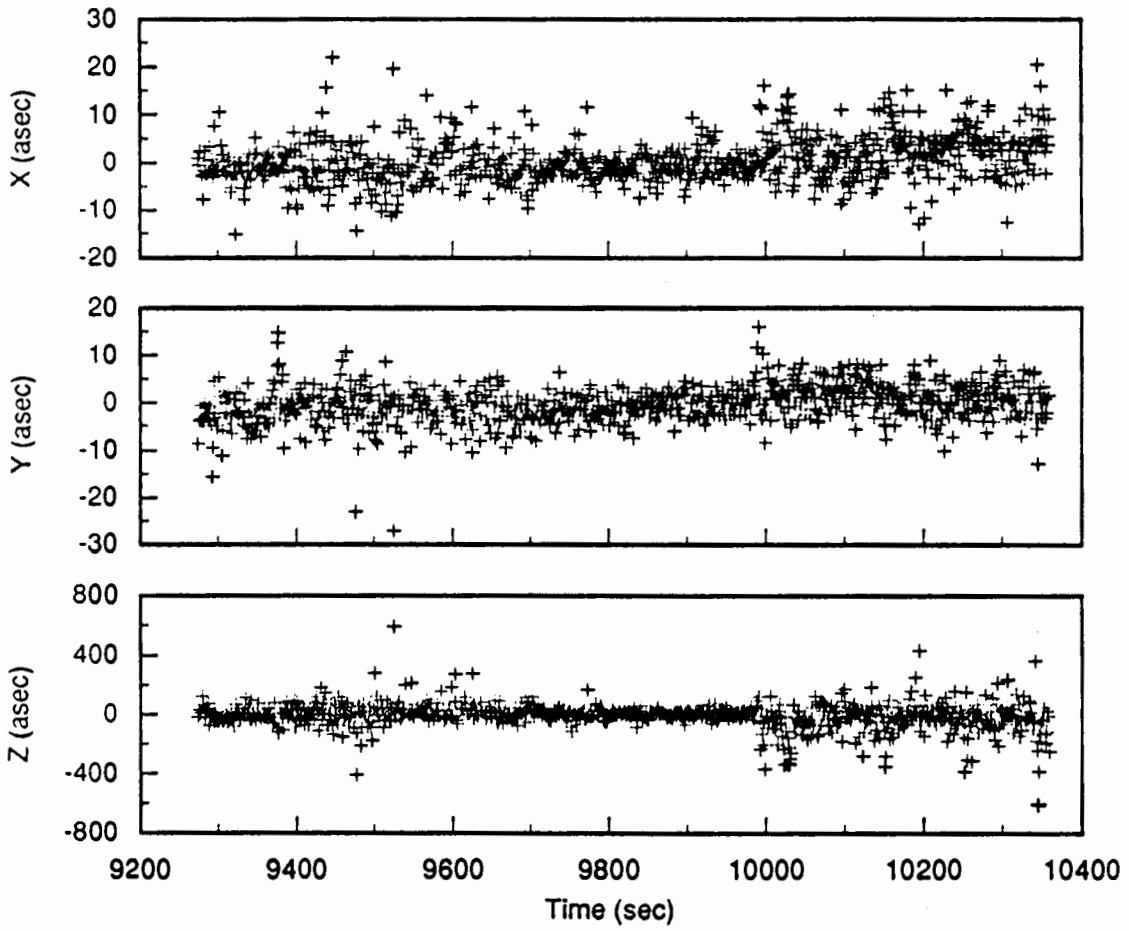

Fig. 5 Single-frame attitude errors for an Earth-fixed case. The errors are smaller in the middle, when a consistent star pattern was observed.

SUMMARY OF TEST RESULTS

Star Position Accuracy

The test data reveal much of the fine structure of star position errors. There are several sources of error which likely dominate. One is the quantization error (eight bits) of the camera's analog-to-digital converter for the CCD readout. This is the dominant error for faint stars. Another source is the interpolation error, which is a function of the image location with respect to the pixel and of star image size and shape. There may also be large spatial-frequency errors due to the limited precision in the lenticular radial-distortion correction. In addition, the calibration is applicable to only one particular spectral distribution, stars of different spectral type requiring different corrections. There is also a temporal error caused by photon and electronic noise in the system. Some of these errors are sensitive to the specific camera design and will be improved as the design matures.

There are other contributions to the residuals besides camera measurement errors. Biases in the residuals may be due to catalog errors. Uncompensated motion of the camera, caused by telescope drive errors for example, also add to the residuals. However, this can be detected by looking for correlation between the residuals of all the stars in the FOV. Atmospheric refraction also contributes to the star

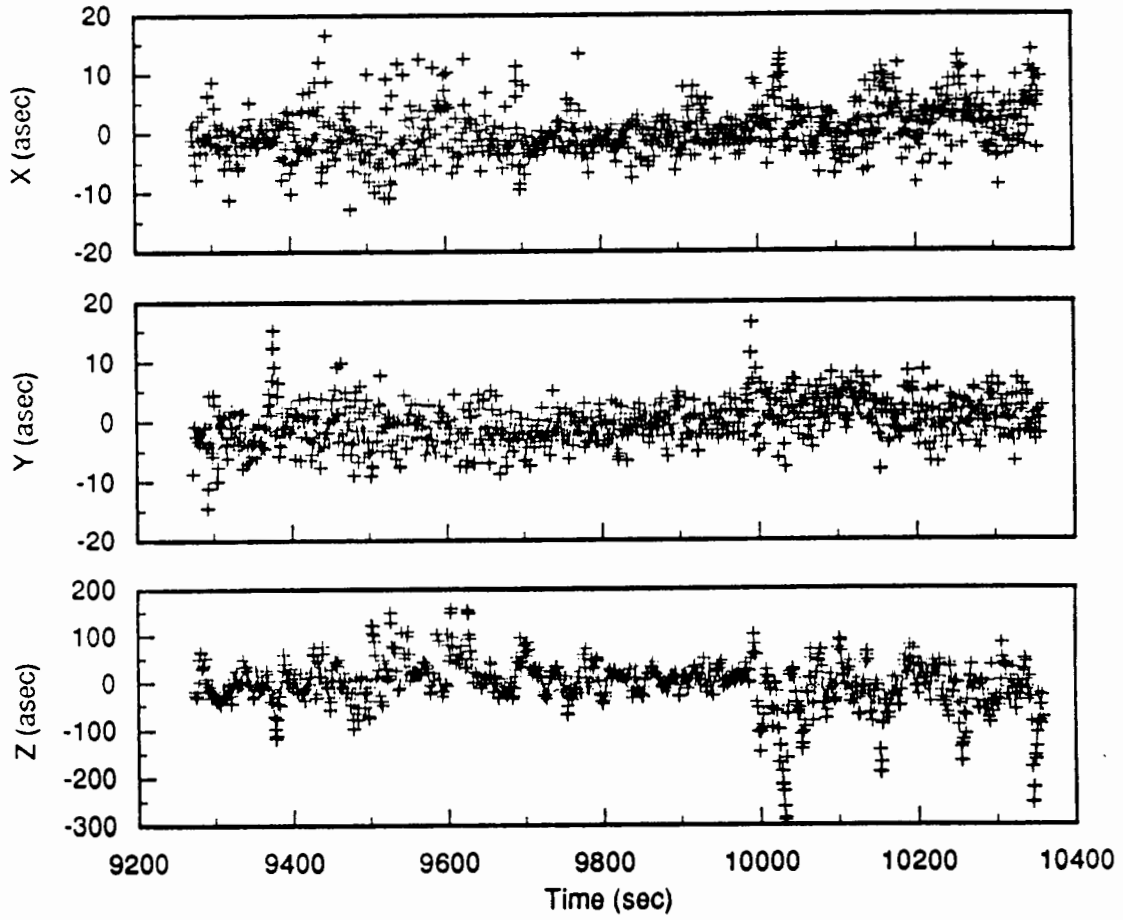

Fig. 6 Kalman-filter attitude errors for an Earth-fixed case. The roll (z) errors show the greatest improvement over the single-frame results shown in Fig. 5.

position error and is as yet uncompensated. Total refraction varies from zero at the zenith to about 35 arc seconds at a zenith angle of 30 degrees. Differential refraction within the FOV could cause biases in the residuals. Changes in total refraction due to changing optical path length as a function of star camera elevation may have more complicated effects.

From a large number of observations and conditions, we have developed an accuracy versus magnitude relationship, shown in Fig. 8. Each point represents the standard deviation of the residuals for a single star from a single data segment (since the stars were not all measured an equal number of times, each point represents different amounts of data). The fainter stars have larger errors, as expected. The ordinate of Fig. 8 is instrument magnitude as determined from CCD spectral response. An approximate visual-magnitude scale can be made by adding 0.5 to the instrument magnitude. The stars were attenuated by atmospheric extinction and absorption by the enclosure window and would appear brighter in space by about 0.30–0.35 magnitudes. Thus, the position errors associated with observations *in space* in stars of fifth to sixth magnitude would be reduced by 3 to 4 arc seconds.

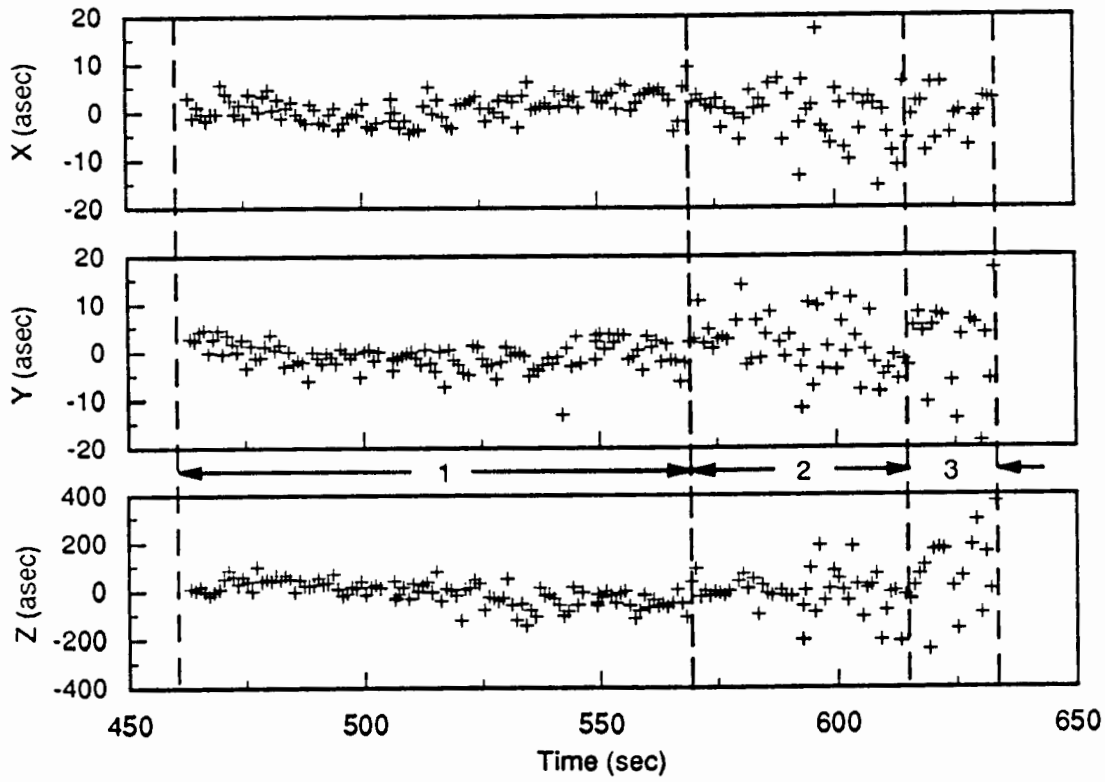

Fig. 7 Single-frame attitude errors for a 0.1 deg/sec slue. The larger errors at the end are caused by a rapidly changing star pattern.

Attitude Accuracy

The single-frame attitude accuracy is determined by the size of the errors of the individual stars in the frame. Ideally, the attitude accuracy about the two axes orthogonal to the boresight should be greater than the individual star accuracy by a factor equal to the square-root of the number of stars used to compute the attitude. As can be seen from the cases discussed here, individual position errors were about 5 to 15 arc seconds, depending on the star brightness, while the single-frame attitude accuracy, when using 3–5 stars, was about 4–5 arc seconds about the x- and y-axes. Obviously, there are many systematic errors which may affect this rule but these tests verify the power of the overall technique of using multiple stars for attitude determination.

Our tests also indicate additional improvement is possible by filtering the single-frame attitude estimates, particularly in roll. However, it is more difficult to quantify this and we have not processed a sufficient quantity of data from which to draw meaningful conclusions.

Camera Improvements

The frame-to-frame attitude "jitter" evident in several of the cases discussed above could be reduced in some cases if the camera tracked the same stars across the FOV rather than selecting five stars on its own. The present algorithm sometimes produced a frequently changing star pattern; consequently, different systematic position errors for each star will produce jitter in the attitude solution. Ensuring that "good" stars are tracked, however, would probably require that the instrument processor, with

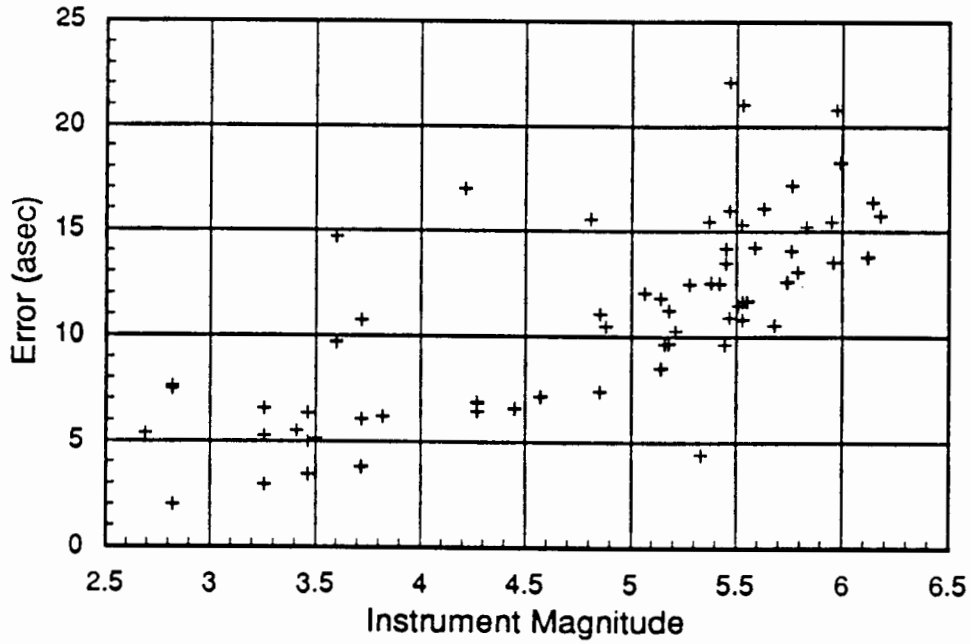

Fig. 8 Distribution of total position error for stars measured in these tests.

access to the star catalog and knowledge of the spacecraft rates, determine which stars to track; this obviously requires additional processing and real-time control of the camera.

We have detected larger position errors as stars near the edge of the FOV. We have not yet determined the cause, but in any case, one simple solution would be for the camera processor or our data-processing software to delete stars near the edge from consideration.

A number of improvements in camera design are possible. Cameras will use CCD arrays of larger format, higher resolution analog-to-digital converters, and more powerful processors.

Future Tests and Analysis

Only a small amount of data from our tests has been processed to the level discussed in this paper. Although we have learned a great deal, there are other cases, such as other slue rates and extinction data, which may provide insight for performance we might expect in a space experiment.

One refinement we will incorporate is correction for atmospheric refraction in our data-reduction software. We have the information needed (time and angles) to compute the mean refraction correction, which should be sufficient for our needs, but not the temperature and pressure for higher-accuracy correction.

The instrument star catalog can be validated using the test data. There were several instances of detected stars that apparently were not in our catalog or catalog stars that were not detected, even in sparse regions. The catalog was edited to remove faint stars in dense regions and to remove closely spaced doubles that would cause confusion in the star identification process; this editing should be verified.

As star cameras improve in accuracy, more accurate testing facilities must also be provided. The test methods presented here may also have to be improved and conditions monitored more closely.

Tests with real stars may continue to be a valuable part of testing both the cameras and attitude-determination software.

CONCLUSIONS

The test methods and results presented in this paper demonstrate the value of testing CCD star cameras and attitude determination software with real stars and precision sluing. Earth-fixed and sluing tests provide a measure of camera performance that is difficult or impossible to produce in the laboratory. Frame-to-frame position errors can be detected very easily as stars move slowly through the field of view. Bias and larger spatial errors can also be detected. We have shown that it is possible to identify stars and determine attitude accurately in a variety of conditions. Attitude accuracy is improved by using multiple stars in each frame, increasing the accuracy, in our case, from 5–15 arc seconds, for a single star, to 4–5 arc seconds. for a stationary or slowly moving camera.

Our methods for testing worked very well. The Earth-fixed tests require limited test equipment: the camera, an enclosure and stable mount, data-collection computer, and a dark, clear site. Sluing tests require, in addition, a precision platform such as an observatory telescope or rotary table.

ACKNOWLEDGEMENTS

The research and development reported here were carried out under contract to the US Army Engineer Topographic Laboratories, Fort Belvoir, Virginia. The support and encouragement of Connie Gray is gratefully acknowledged. We are grateful to Allan Eisenman of JPL and the staff of JPL's Table Mountain Facility for their assistance during our tests.

REFERENCES

1. GRAY, C., and STRIKWERDA, T. E. "Satellite Attitude Determination Using a CCD Star Camera," *Annual Convention of the Am. Congress on Surveying and Mapping and Am. Soc. of Photogrammetry and Remote Sensing*, March 1988.

2. STRIKWERDA, T. E., and FISHER, H. L., "A CCD Star Camera Used for Satellite Attitude Determination," Proceedings, Summer Computer Simulation Conference, Seattle, Washington, July 1988.

3. JUNKINS, J. L., and STRIKWERDA, T. E., "Autonomous Star Sensing and Attitude Estimation," *Rocky Mountain Guidance and Control Conference*, Paper AAS 79-013, February 1979.

4. BLACK, H. D., "A Passive System for Determining the Attitude of a Satellite," *AIAA Journal*, Vol. 2, No. 7, pp. 1350–1351, July 1964.

5. SHUSTER, M. D., and OH, S. D., "Three-Axis Attitude Determination from Vector Observations," *Journal of Guidance, Control and Dynamics*, Vol. 4, No. 1, pp. 70–77, Jan- Feb, 1981.

6. FISHER, H. L., SHUSTER, M. D., and STRIKWERDA, T. E., "Attitude Determination for the Star Tracker Mission," *AAS/AIAA Astrodynamics Specialist Conference*, Paper AAS 89–365, August 1989.